



Integrated Well-Site Chemostratigraphy for Real-Time Reservoir Navigation and Geosteering in the Offshore Niger Delta

¹Ihunda, C. E, ²Selegba Abrakasa, ³Soronnadi-Ononiwu, G. C.

^{1,2,3}Department of Geology, University of Port Harcourt, Choba, Port Harcourt

*Corresponding Author ihundaeze@gmail.com

DOI : <https://doi.org/10.55248/gengpi.6.0825.3026>

ABSTRACT

Chemostratigraphy is a means of correlating mixed siliciclastic and carbonate constituents within the stratigraphic profile of sedimentary succession on the basis of variations in concentrations of specific minor, major, trace, and rare earth elements. Recently developed technology now provides the ability to determine concentrations of selected minor, major and trace elements in ditch cuttings collected on the surface of a well site within minutes after the sample reaches the surface. The confidence in stratigraphic positioning of the bit is enhanced by comparison of data acquired during the ongoing drilling process with measurements of offset wells that have been drilled in the past. The offshore study wells are those of the Niger delta of the offshore sandstone in which successful completion of the well depends on landing the casing point in the lower few metres of the Tertiary. The article shows how a borehole can be traced in relation to a chemostratigraphic scheme. After a stratigraphic geochemical characterisation has been established, one can track a borehole when drilling other wells. This research consists of description of the Tertiary overburden succession in wells, and correlations to the same. A real-time correlation framework can also be updated on a regular basis through the use of chemostratigraphy. Of greater significance in drilling terms in this play drilling-wise, valuable geochemical variations can be perhaps pinpointed in the Tertiary shales just above the Sandstone.

Keywords: drilling, characterization; elemental chemostratigraphy; well-site inorganic geochemistry; siliciclastic and Niger Delta

1. Introduction

Elemental chemostratigraphy technique has been applied over the past decades. Usually, it employs the recognition of tiny variations in the entire detrital elemental composition of sedimentary rocks, which is known as chemostratigraphy. These variations are also employed in the subdivision and correlation of the sequences of sedimentary ones. The method can potentially provide geochemical fingerprints to individual formations, groups of sedimentary rock packages forming a formation, where complexities resulted in name mismatching complications in correlation attempts and in many instances necessitating the definition to lithostratigraphy, biostratigraphy and invariably chemostratigraphy (Mazzullo *et al*, 2013, Childress and Grammer, 2015) and, in some cases, individual beds. Amidst the extensive work and suggested geological interpretations there is little published literature in the Niger Delta whereby chemostratigraphic tests are opposed against physical chronostratigraphic testing (North *et al.*, 2005). A popular feature of Geochemistry is chemostratigraphy that gained its popularity in the 80s, but the first article was published in 1986 (Ramkumar, 2015). It involves the fact that sediments have been the record keeper of changes in physical, chemical, biological conditions and events occurring before, during and after their depositions to reflect paleoclimatic changes, tectonic settings, provenance, reservoir properties, paleo-environment; with regards to their source and mechanism linked to their origin in stratigraphic association (Ramkumar, 2015). Prundeanu *et al.*, (2021) applied a novel method of chemosteering (or elemental geochemistry analysis) as one of the alternatives in identifying Cenomanian, Turonian-Coniacian-Santonian, Campanian and Eocene layers. This allowed the accurate location of the horizontal development wells in the sought out reservoir interval. Mejia *et al.*, (2018) used LWD azimuthal resistivity to steer and land wellbore successfully in the reservoir and also check distance-to-bed boundary to cap rock. The reservoir formation with low contrast resistivity and low natural resistivity would allow the advance cuts analysis to enable steering to be made within the variation of the microscale elements ratio and abundance levels. This work seeks to examine and justify the application of chemostratigraphy as the foundation to make a correlation of the ratio of trace metals using the data obtained due to ditch cutting of fluvial reservoirs.

1.2 Location of Study

The study area are located in three depobelts in the Niger Delta offshore, the Depobelts with geographic co-ordinates of latitudes 5°33' 42.533" N to 5°6'21.334" E longitude for DS while ML 1 lies between latitudes 5°46' 42" N to 4°48' 50" E longitude and ML 2 fall within latitudes 5°50' 48" N to longitude 4° 49' 52" E as shown on the map below (Figure 1).

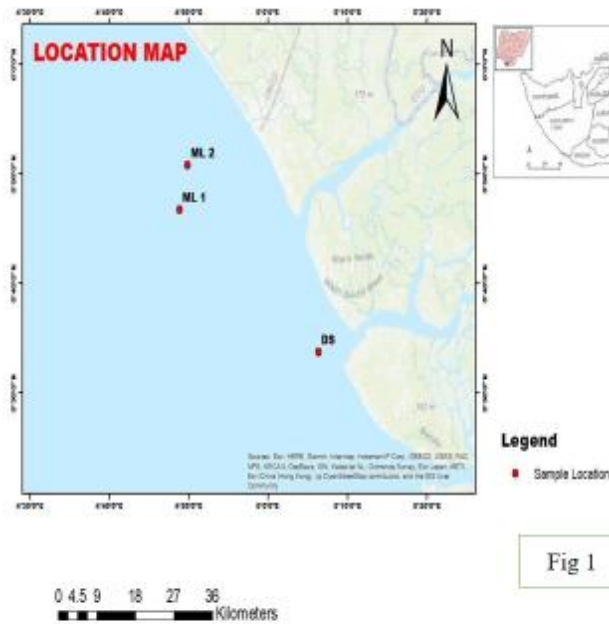


Figure 1: Showing Location Map of the Study Area.

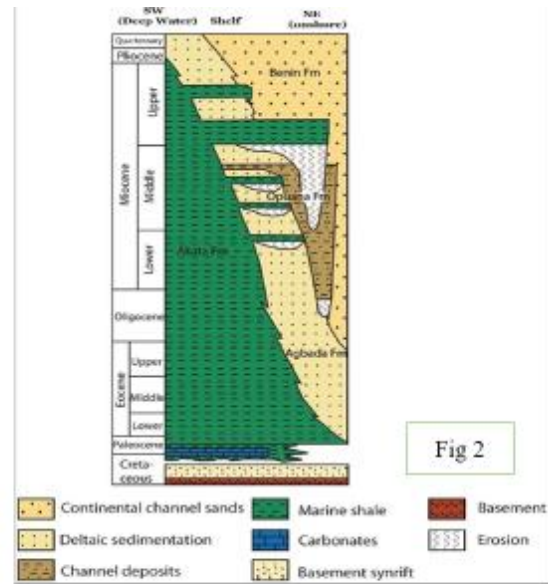


Figure 2: The regional stratigraphic column of the Niger delta Basin shows the three major units in the delta (Akata, Agbada, and Benue formations) (Doust and Omatsola 1990).

1.3 Geology and Stratigraphy

The Niger Delta has a stratigraphic succession of coarsening upwards sequences of diachronous sediments (Weber *et al.* 1975, Evamy *et al.*, 1978). The different depositional environments are the direct cause of the Cenozoic Niger Delta Stratigraphy. Initial news of known facts of a Niger Delta geology were published (Frankl *et al.*, 1967, Short. and Stauble, 1967 and Avbovbo *et al.*, 1978) as well as later works (Evamy *et al.*, 1978, Ejedawe *et al.*, 1984, Haack, *et al.*, 2000 and Reijers, 2011). Stratigraphically the delta can be split up in three formations being the Akata, the Agbada and the Benue formations (Reijers, 2011). These formations are older, basin-ward, because of the overall regressive nature of the depositional environments in the Niger Delta clastic sedimentary wedge (Figure 2).

2. Materials and Methods

This study was conducted on three boreholes wells, which were known as DS, ML 1 and ML 2 well. The study samples were selected well so that they fit within the age range.

A total of 15 samples were analyzed geochemically (major and trace element analysis) at the National Geosciences Research Laboratories at Barnawa, Kaduna. This includes 15 samples of the study well (Sample numbers are well depth on ft). The methods used are multi-acid analysis ICP-MS (MA250) and whole rock Lithium Fusion ICP finish (LF300). Most of the minerals can be dissolved using the MA250 approach. The procedure was carried out using 15 samples. A split (0.25 g) is fused in HNO₃, HClO₄ and HF and dried, and any remaining solid dissolved in HCl. In the LF300 (ICP/ICP-MS) analysis, the analysis uses the fusion method to decomposes even the hardest of matrices in its entirety to determine the level of the major oxides and loss on ignition (LOI) concentration. This was done in all the 15 samples. The sample was also split in order to represent the overall sample and these were used to make quality (QA/QC) control checks as the analytical part was being carried out progressively. The figures were also used to compare the stated concentrations with the Post Archaean Australian Shale (PAAS, Taylor and McLennan (1985)) and also with the mean concentrations of the Upper Continental Crust (McLennan, 2001). The above discussion and the fact that the key geochemical characteristics of the beds at and above the ideal casing point were identified before conducting the well-site analysis enabled accurate selection of casing point at the well-site in all wells in the drilling program.

3. Results and Discussion

Regional chemostratigraphy

The elements and element ratios plotted as chemical logs for three vertical study wells in Figure 3, which allows the study interval to be divided into 4 chemostratigraphic zones units, the main features of which are the profile consists of log view throughout the well for V/Ni, Y/Nb, Zr/Cr, Rb/Cs, Cr/Na₂O, Na₂O/Al₂O₃, Ga/Rb, Al₂O₃/Bases and (Fe₂O₃+MgO). Shale volume implies a sandstone formation that is 12,300 ft to 13, 500 ft, followed by the intercalations of shales, sandstones, siltstones and carbonate rocks 7,840 ft to 8, 660 ft in the ML 1 well is composed predominantly of carbonate rocks and 13,240 ft to 14, 530 ft in the ML 2 well in the well. Fe₂O₃/SiO₂ is also poor (0-16) within the identical time span at the foot of the wells as a

result of low occurrence of organic matters and comparative development of pyrite. But between the middle and topmost levels of the three Wells the Ti/Zr will diminish (5-65) and Fe/S will increase (4-45) on the same proportional ranges in the 3 wells (Figures 3-4). Going by these features, Table 1 below is the overview of the concentration of the major oxides of the wells.

Table 1. Trace/ Minor Elements of DS, ML 1 and ML 2 Well for Chemostratigraphic Characterization

Elements (ppm)	DS					ML 1					ML 2				
	12300	12630	12940	13290	13500	7640	8060	8220	8440	8660	13240	13510	13720	14140	14590
V	9840	5600	8400	9740	4200	184	434	306	2900	421	1101	9489	9488	9490	9840
Cr	380	1800	2200	240	700	500	500	800	1600	800	500	2500	4100	3050	2400
Ca	62	800	1300	3000	460	40	500	400	620	600	1000	800	800	300	1100
Sr	460	288	401	3600	211	201	430	240	500	340	302	560	500	430	510
Zr	<0.001	9890	9610	310	8010	<0.001	<0.001	<0.001	9600	<0.001	9100	9200	8900	8850	6500
Ba	201	400	400	220	334	264	320	160	330	240	430	390	124	510	2500
Zn	80.00	500	512	<0.001	500	244	240	181	500	<0.001	1600	2.01	1600	3050	3200
Cu	<0.001	<0.001	<0.001	<0.001	<0.001	<0.001	<0.001	<0.001	<0.001	<0.001	0.21	<0.001	<0.001	<0.001	<0.001
Pb	0.78	<0.001	<0.001	<0.001	<0.001	<0.001	<0.001	<0.001	<0.001	<0.001	9301	9810	9789	9840	9811
Bi	<0.001	<0.001	<0.001	<0.001	<0.001	<0.001	<0.001	<0.001	<0.001	<0.001	<0.001	<0.001	<0.001	<0.001	<0.001
Ga	18.5	18	<0.001	<0.001	18.5	22.5	20.55	20	24	21	19.4	0.84	21.2	14	18.5
As	<0.001	1.16	18.5	<0.001	0.95	38	<0.001	0.021	0.64	<0.001	<0.001	<0.001	<0.001	<0.001	1.95
Nd	<0.001	<0.001	<0.001	<0.001	<0.001	<0.001	<0.001	<0.001	<0.001	<0.001	<0.001	<0.001	<0.001	<0.001	<0.001
Y	<0.001	<0.001	<0.001	<0.001	10	<0.001	<0.001	0.7	0.84	<0.001	2	<0.001	<0.001	<0.001	1.2
Ni	3600	<0.001	110	4300	<0.001	300	<0.001	400	<0.001	600	<0.001	<0.001	400	<0.001	<0.001
Rb	0.48	3	0.008	<0.001	<0.001	0.11	0.65	<0.001	0.12	2	0.062	<0.001	12	0.04	0.08
Mo	6900	3410	5600	5700	1200	1500	1800	150	1400	500	1230	1200	2400	1000	900
Ti	<0.001	<0.001	<0.001	<0.001	<0.001	<0.001	<0.001	<0.001	<0.001	<0.001	<0.001	<0.001	<0.001	<0.001	<0.001
Cd	0.06	<0.001	<0.001	<0.001	<0.001	<0.001	<0.001	<0.001	<0.001	<0.001	<0.001	<0.001	1.04	<0.001	<0.001
Ru	<0.001	1.41	<0.001	<0.001	1.33	<0.001	<0.001	<0.001	1.27	1.81	0.7	<0.001	1.04	0.65	0.71
Eu	0.12	<0.001	<0.001	<0.001	<0.001	<0.001	<0.001	<0.001	<0.001	<0.001	<0.001	<0.001	<0.001	<0.001	0.06
Rh	19.21	21.24	25.07	40.31	35.09	25.2	25.23	26.08	40.21	32.02	22.1	24.33	27.65	40.35	30.08
Re	<0.001	<0.001	<0.001	<0.001	<0.001	<0.001	<0.001	<0.001	<0.001	<0.001	<0.001	<0.001	<0.001	<0.001	0.12
Nb	3400	<0.001	0.28	3400	<0.001	500	<0.001	600	700	<0.001	<0.001	<0.001	<0.001	<0.001	0.4
Ta	500	<0.001	1.001	461.00	<0.001	321	<0.001	430	1000	<0.001	<0.001	<0.001	<0.001	<0.001	0.02
W	112.00	<0.001	24	32	<0.001	6.6	<0.001	20	23	<0.001	<0.001	28	1900	0.14	0.81
Hf	<0.001	23.5	31	<0.001	26	<0.001	<0.001	40	46.5	<0.001	32	<0.001	28	52	60
Yb	<0.001	<0.001	<0.001	<0.001	<0.001	<0.001	<0.001	<0.001	<0.001	<0.001	<0.001	<0.001	<0.001	<0.001	<0.001
Se	<0.001	<0.001	<0.001	<0.001	<0.001	<0.001	<0.001	<0.001	<0.001	<0.001	<0.001	<0.001	<0.001	<0.001	<0.001
U	<0.001	<0.001	<0.001	<0.001	<0.001	<0.001	<0.001	<0.001	<0.001	<0.001	<0.001	<0.001	<0.001	<0.001	<0.001
Th	<0.001	<0.001	<0.001	<0.001	<0.001	<0.001	<0.001	<0.001	<0.001	<0.001	<0.001	<0.001	<0.001	<0.001	2
Sb	<0.001	<0.001	<0.001	<0.001	<0.001	<0.001	<0.001	<0.001	<0.001	<0.001	<0.001	<0.001	<0.001	<0.001	<0.001
Ge	21.5	<0.001	12.05	<0.001	6.5	12.05	<0.001	20	18	12	10.64	13.5	<0.001	14.5	28
Sn	168	33	34	9840	0.084	34	16	140	200	<0.001	1.062	110	210.00	210	790
Pd	<0.001	0.84	<0.001	<0.001	0.77	<0.001	<0.001	<0.001	0.58	<0.001	1.6	1.85	0.48	<0.001	0.22
La	0.118	<0.001	<0.001	<0.001	0.03	<0.001	<0.001	<0.001	0.76	0.002	<0.001	<0.001	0.12	2	3.6
Co	<0.001	0.14	<0.001	<0.001	0.17	<0.001	0.09	<0.001	1.9	0.99	0.14	0.2	0.01	0.07	0.17

3.1 Chemostratigraphic Weathering Stability for ML 1 Well

DS Well

The plot of different log view diagram of kaolinite versus Al_2O_3 presented below denotes a weak linear correlation with a K_2O (Figure 3a). This implies that additional Al_2O_3 laden minerals may as well have played the role of distributing Al_2O_3 in DS well. The presence of K_2O in DS well was regulated by involved minerals that were more than one. To give an example mentioned in the Table 2, microcline, illite/ muscovite and jarosite caused the distribution of K_2O in the DS well; however, microcline had a greater influence on K_2O distribution than other minerals containing K_2O .

Because of the significance of this casing point, about three explorations were analysed in the laboratory. Silt claystones, which are immediately over 12,550 ft indicated an enrichment in the Si, Ca and Zr and depletion in Ti and Al. These are unique and recurrent in the three of the control wells. In sample 12,300 ft; marks an increase in Al_2O_3 with a little decrease in K_2O sandstone and also an increase abundant in Al_2O_3 within depth 12,700 ft to 13,100 ft which is equivalent to K_2O at 12,700 ft and these elemental mineral is also presence within these depths (Figure 3a); but a massive decrease in K_2O and Al_2O_3 but also an abundant increase in Zr and a gradual decrease in P_2O_5 down dip the hole.

Table 2: Major oxides for chemostratigraphic characterization of DS Wells

Oxide composition (%) DS												
Depth (ft)	SiO ₂	MgO	CaO	K ₂ O	Na ₂ O	MnO	P ₂ O ₅	Fe ₂ O ₃	TiO ₂	Al ₂ O ₃	SO ₃	H ₂ O
12300	5.06	ND	ND	ND	ND	0.77	0.68	53.08	ND	8.00	4.01	27.60
12630	51.80	ND	ND	ND	ND	0.18	ND	0.38	5.18	12.00	3.16	21.30
12960	48.54	ND	0.02	1.20	0.60	0.36	0.34	6.10	2.74	17.51	ND	22.60
13290	4.20	ND	ND	ND	ND	0.95	0.05	67.90	ND	2.48	ND	24.50
13500	49.13	ND	ND	0.46	0.12	0.18	ND	6.12	4.76	12.48	3.76	22.80

Table 3: Major oxides for chemostratigraphic characterization of ML 1 Well

Oxide composition (%) ML 1												
Depth (ft)	SiO ₂	MgO	CaO	SO ₃	K ₂ O	Na ₂ O	TiO ₂	MnO	P ₂ O ₅	Fe ₂ O ₃	Al ₂ O ₃	H ₂ O
7840	46.08	ND	ND	ND	1.10	0.60	3.38	0.17	0.43	6.18	24.42	17.00
8060	48.27	ND	ND	0.82	0.30	0.02	3.92	0.23	0.20	0.38	18.46	14.40
8220	47.14	ND	ND	2.73	ND	ND	3.53	0.09	0.48	7.00	23.70	15.10
8440	47.80	0.65	1.00	1.52	0.20	0.02	4.32	0.20	ND	17.02	12.48	14.60
8660	48.27	ND	ND	0.82	0.30	0.02	3.92	0.23	0.20	13.06	18.46	14.40

Table 4: Major oxides for chemostratigraphic characterization of ML 2 Well

Oxide composition (%) ML 2												
Depth (ft.)	SiO ₂	CaO	MgO	SO ₃	K ₂ O	Na ₂ O	TiO ₂	MnO	P ₂ O ₅	Fe ₂ O ₃	Al ₂ O ₃	H ₂ O
13240	37.53	1.06	0.59	4.96	0.50	0.18	10.44	0.61	ND	17.01	13.90	13.00
13510	48.08	ND	ND	4.73	ND	ND	13.73	0.45	ND	10.43	8.00	16.50
13720	51.88	1.00	0.18	3.75	ND	ND	14.07	0.45	ND	19.00	3.15	6.50
14140	24.79	ND	ND	7.23	ND	ND	22.52	0.69	ND	25.08	6.89	12.40
14530	31.16	ND	ND	5.81	ND	ND	13.63	0.60	ND	26.18	9.62	12.80

ML 1 Well

The oxygenation of the bottom water, as indicated by the vanadium enrichment factor (EFV) decreases with depth across the section (Figure. 3b), as indicated by Uranium (U) and phosphorus oxide (P₂O₅), there is also a possible reduction in the organic matter/biogenic probably to indicate a gap in sedimentation or unconformity (Ratliffe et al., 2012). No biogenic productivity (no P₂O₅ log kick recorded) or terrigenous supply is recorded at this interval (7,840-8060 ft). The range 8,060-8,440 ft (Fig. 3b) is a high biogenic productivity (high P₂O₅ log), optimal and modification in oxygenation of the bottom water of formation. It is also the time interval of maximum fossils (as indicated by large kick of the U-log and of the Mo logity (largely due to upsurge or biogenic productivity and supply of terrigenous material at 8,220 ft, and this elemental mineral is also retained within these depths; but a massive decrease in K without upsurge in Al Ca and Si enrichments are a reflection of the reworked sediments respectively (Table 3). Heavy mineral namely, zircon maintains Zr enrichments. Concentrations of Zircon is characteristic of a winnowed lag deposit. Al and Ti also reduce with loss of clay minerals and the micas with winnowing. The ditch cuttings samples of the basal tertiary cannot be easily distinguished with the aid of a binocular microscope even though the samples are clear geochemically. Such differences are unique and are repeated in the control well. In sample 7,840 ft; marks an increase in Al₂O₃ with a decrease in K₂O sandstone which reflect the absence of Zr/P₂O₅ at the same depth and also an increase abundant in

Al₂O₃ within depth 8,060 ft to 8,440 ft but a total decrease in K₂O within the same depth but equivalent to Zr/P₂O₅ at 8,060 ft to 8,440 ft and these elemental mineral is also presence within these depths (Figure 3b); but a massive decrease in K₂O and Al₂O₃ but also an abundant decrease in Zr and a gradual decrease in P₂O₅ down dip the hole.

ML 2 Well

The major elements selected to plot for interpretations were detrital proxies (Al, K, Si, Mg, Fe, and S) and phosphate proxies (Ca, Zr, P). In the downhole cutting, there is a major shift in element concentration occurring at 13,240 ft between the shale formation unlike the proposed boundary between the DS and ML 1 wells which record a major significant shift in elemental concentration (Table 4). Figure 3c). In the ML 2 well, there is a gradual increase in terrigenous influx (Al, K, Si, Mg and Fe) with a corresponding decrease in phosphate input (P₂O₅) and a positive increase in Zr until 13,720 ft. This depth marks a shift in elemental concentration from the ML 2 Well into the up section in contrast to the proposed boundary between the ML 2 well (Figure 4.26). This boundary represents basinal changes during deposition.

Since casing point is important, the samples of the base Tertiary of three wells were previously drilled were analysed in the laboratory before collecting data at well-site (Figure 3c), shows that at depth 13,240 ft in the ML 2 well has higher content of K₂O in the sediment and where completely absent in the other depths, but shows an increase in Al₂O₃ down the well, while other samples in the plot has lower K₂O content. In this context, the well casing in this zone should be avoided or handle with improved technology due to high possibility of casing failure, because of erosion (Craigie, 2018).

In Figure 3c, and Figure 4c, shows that at 13,240 ft K₂O content is higher when compare to U (ppm) content which is lower and relative to other sampled depth in ML 2 well. (Ikhane, *et al.*, 2014). Another finding was that, despite being much higher in the number of the detrital heavy minerals, the fluvial facies remains more abundant than their counterparts (ditch cutting facies), and P₂O₅ / Zr profiles are plotted on different scales in each case yet the pattern of this ratio is very similar in nature as indicated that ages of the stratigraphically oldest sediments the fluvial facies are usually characterized by higher Zr value than that of the younger one sections of the ML 2 well.

3.3 Weathering Stability of the Study Wells DS

The geochemical frontier (Figure 4a). Based on the plot of K₂O and U (ppm), there was a general increase and the general increase at 12,960 ft and the average values trending downwards to 12,300 ft; 12,600 ft; 13,290 ft and 13,500 ft show that at 12,960 ft the well will collapse and not conspicuous (Figure 4a). There were greater values of KO₂ (1.05%-2.40%) and lesser values of U (ppm) (0.09%-0.60%) in the plot. Means of KO₂ and U (ppm) values are 2.122 percent and 0.152 percent respectively. It shows that at depth 12,960 ft in the DS Well has more potassium and hence potentially more susceptible to weathering/erosion and could easily result to well failure due to casing collapse, which is the plot of U (ppm) versus KO₂ for DS well, it indicates that at depth 12,960 ft, have higher KO₂ content in the corresponding sediment sample, with approximately similar U (ppm) content relative to other samples in the plot (Figure 4.8). This translates to the greater sediment instability and higher potential for well collapse at 12,960 ft. This should implies that the sandstone formation at depth 12,630 ft to 13,500ft bear poor sweep/production efficiency.

3.4 Weathering stability of ML 1 Well

The plot had higher KO₂ values (0.20% to 1.10%) and lower U (ppm) values (0.0%). The averages of KO₂ and U (ppm) values in were 0.016% and 0.045%, respectively. It shows that depth 7,840 ft in the ML 1 well has more potassium and hence potentially more susceptible to weathering/erosion and could easily result to well failure due to casing collapse. Which is the plot of U (ppm) versus KO₂ for well ML 1, indicates that depth 7,840 ft, have higher KO₂ content in the corresponding sediment sample, with approximately similar U (ppm) content relative to other samples in the plot (Figure 4b). This translates to the greater sediment instability and higher potential for well collapse at 7,840 ft. This ought to mean that the sandstone structure of 7,840 ft to 8,600 ft may find poor sweep/production performance (Figure 4b). But, the sandstone stratum in the lower sequence, have less kaolinite and fewer pore filling minerals in proportion to the improved production efficiency than in the lower series in comparison Figure 4b, shows the plot of ML 1 depth versus KO₂% in sediments of the corresponding depth indicating that depth 7,840ft had more potassium oxide which fosters erosion and hence weathering of the sediments. This in the subsurface, the concept of well placement and stability will result to soil/sediment instability and potential for collapse of well casing. Comparatively, other depths will be more stable than 7,840ft. Figure 4b indicates that depth 7,840ft in the well has higher KO₂ thus more unstable relative to other sample points. However, the other depth points have similar amount of U (ppm).

3.5 Weathering stability of ML 2 Well

The geochemical boulder (Figure 4c). Based on the plot of K₂O and U (ppm), a general increase was evidenced and a distance at 13,720 ft and the values headed downwards 13,240 ft; 13, 510 ft; 13,720 ft; and 13,500 f. Above the geochemical boundary at 13,240 ft, the trends of K₂O and U (ppm) decreases although they were generally large and there was general increasing trend at the base. Therefore, the well will Notwithstanding these distinct geochemical signals, the cuttings sample in the basal Tertiary cannot easily be distinguished, on binocular microscope observation, with respect to the Tertiary sequences that overlie it. Figure 4c, shows that depth 13,240 ft in the ML 2 has higher content of K₂O in the sediment, while other samples in the plot has lower K₂O content. In the context of well casing that zone should be avoided or handle with improved technology which is similar to 13,240 ft has higher K₂O content but similar U(ppm) content relative to other sampled depth in well ML 2 well.

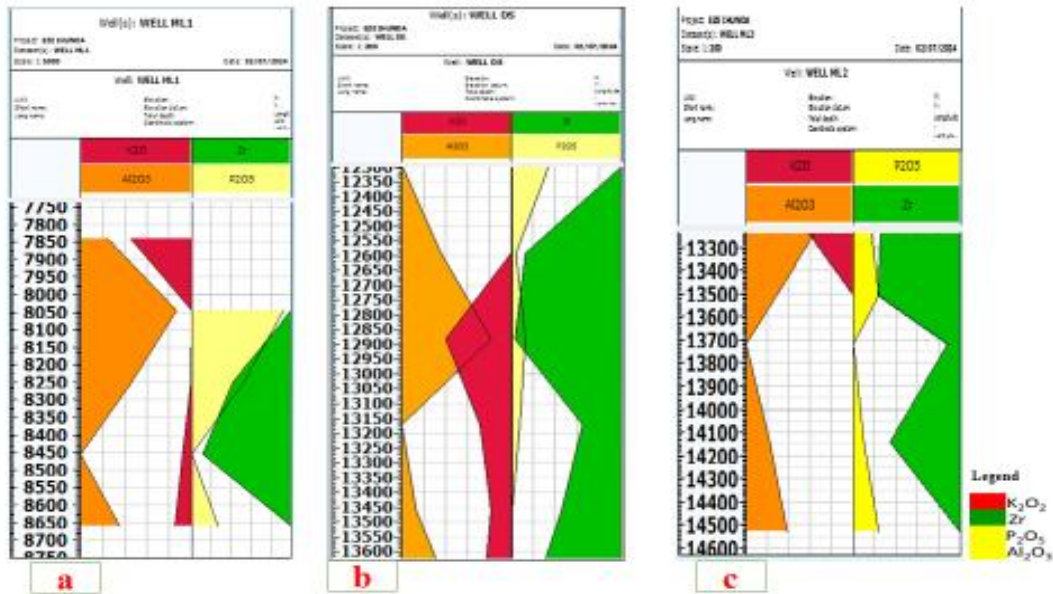


Figure 3a-c: Showing depiction of various log view of DS, ML 1 and ML 2 Well

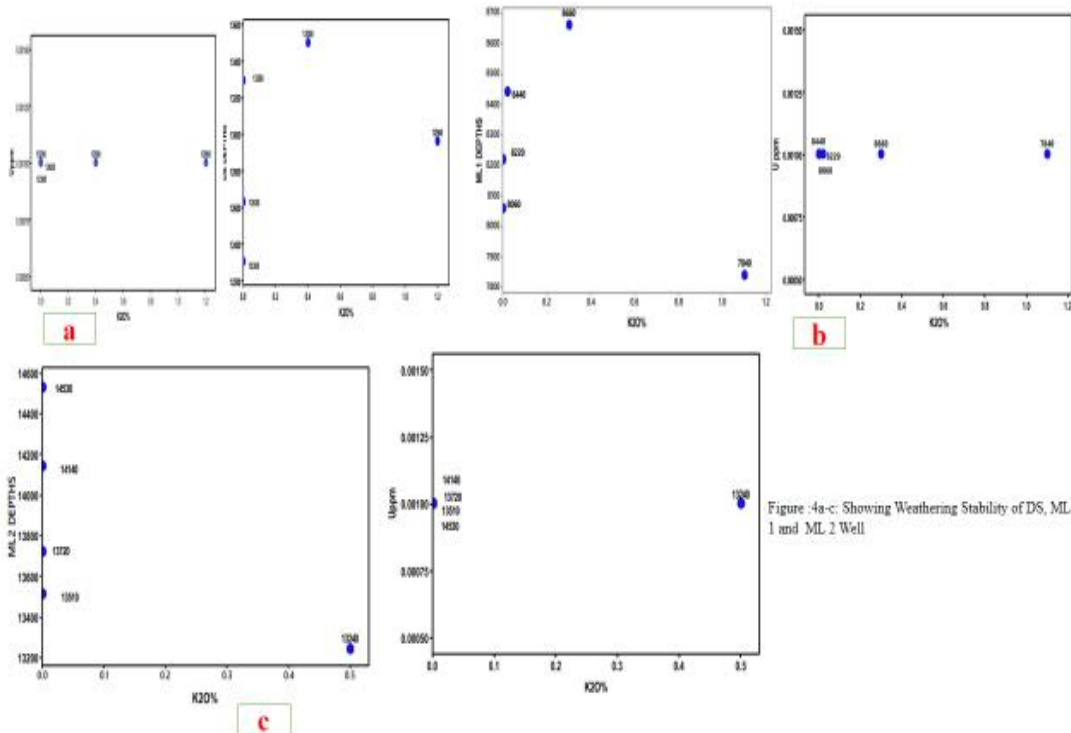


Figure 4a-c: Showing Weathering Stability of DS, ML 1 and ML 2 Well

3.6 Chemostratigraphic Correlation of the Study Wells

An inorganic geochemical correlation of the three wells was established; this correlation had nothing to do with geology or mineralogy (Figure 5). Hence, there was a necessity to know the probable mineralogical control on these geochemical key elements based on which the correlation was applied. Through this, more geological facts were established through the correlation which was founded on inorganic geochemistry. Also, the identification of the minerals that regulate the key components made it easy predict the mineralogical controls involved in the geochemical key element differentiation; therefore, it aided in the interpretation of the stratigraphic layers.

Figure 5 and 6 presents the summary of the chemostratigraphic correlations with the geochemical profile of ratios of some values observed between the wells under studies. The preparation of the correlation scheme begins with plotting of all elemental data in a profile. The sample distribution can also be assessed within the combination of binary and ternary diagrams of the elements and ratios where variation within the depth profile is observed. Next, comes identification of the important components and elemental ratios which enable tags the differentiation of the MZ 1, MZ 2, MZ 3 and MZ 4 zones with great zonation confidence. The three wells correlation scheme suggested is high, and more than 85 percent zonation confidence is obtained. The

four geochemical zones can be identified by all the three wells (DS, ML 1, and ML 2), which indicates an accurate correlation scheme to the study wells. The transparency between the line curves of the ratio of elements and elemental assists in seeing the correlation log of the three offset wells better. The variation of shading colour or area is, as a rule, signifying a change of zone (Figure. 5). As a rule, variability of the geochemical composition of the zones in the three wells are similar. The layer MZ 1 reflecting the lower layer of the Miocene formation and is similar in each of the three wells. An additional zone, MZ2, above the reservoir, spills over the Early-and Late Miocene and over the so-called Shale series of the Early- Late Miocene, showing a typical down hole pattern of Sr/Cr variation, in the form of an inversion with depth. This is an extremely critical variable because it gives information on well trajectory position ahead of time causing more appreciate the positioning in regards to the reservoir interception. Zone MZ 4 is characterized by silt, sandstone/quartzitic sandstone and there is a slight (yet definitive) increase in the carbonate content in the (East-West) EW direction. On the top of zone MZ 4, a positive excursion of Cr/Zr ratio is seen in all the offset wells, Sr/ Cr ratio took its downhole decreasing trend and attained its minima in this zone. Most often, the correlation is layercake in nature with minimal differences between wells. Zone MZ 3 (Miocene), accumulated in a syn-rift tectonic environment, can be traced unequivocally by a geochemical fingerprint using which the correlation between the wells under study was determined (Figure. 6). Mo/Sr and Hf/Ge have a dim visible rise at top of zone ML 3 and V/Ni and Sr/ Cr have strong negative excursion.

3.7 Chemostratigraphic Correlation of Long range of the DS ML 1 and ML 2

The well features the oldest part, which includes fine lithologies of low Cr/Zr and Sr/Cr values plotting in relation to zones in the field (Figure. 5). A great increase in values of the Cr/Zr and Sr/Cr ratios is observed 13500 ft above the base of the section that is correlated to the same feature in ML 1 and ML 2 section that defined the top of magezone 1. This is evidenced by the alteration in the composition of the coarse lithologies in both sections which occur at 13500 ft above this surface in the DS section and ML 2 section. An abrupt increase V/Ni values of the fine grained lithologies enables the identification of the top of magezone 2 in the two sections. It is supported by the binary diagrams that coincide with the assignment of samples to magezone 2. Fine grained lithologies of magezone 3 have V/Ni values that stand out as low and Cr/Zr values as high in both sections. The top of the magezone is near enough to the top of the study interval in the ML 2 section that it can be determined fairly precisely by the increasing trend in Cr/Zr and Sr/Cr ratios upwards. This shift may be made in a zone of no exposure in DS (Figure. 5). Coarse lithologies at the base of magezone 4 in the DS section comprise very high Cr/Zr values, and similar composition was observed at the base of this magezone in the ML 1 section, no coarse lithologies were analysed at magezone 4, at ML 2 section. The DS section projects nearly 300m stratigraphically over the top of the ML 2 section

3.8 Chemostratigraphic Correlation of Short range of the DS and ML 2

The lithologies of the ML 2 section occur as fine lithologies that can be identified as three distinct clusters in binary diagrams thus enabling the magezone within the ML 2 section to be identified in the DS section (Figure. 6). Besides this correlation of magezone, magezone 3 is subdivided into four geochemical units (30-50 m thick) and are correlative between the ML 2 and DS well sections, with high V/Ni values that seems to be transitional magezone 2 to the above units of magezone 3. Magezone 1 is typified with low Mo/Sr values as compared to the rest in the magezone 3. Magezone 2 contains high values of Hf/Ge and Sr/Cr compared to magezone 4 and 3, respectively. Magezone 1 with high value of V/Ni remains only in the DS well interval and is likely to be related to a zone of zero exposure interval recorded in the ML 1 well (Figure. 6).

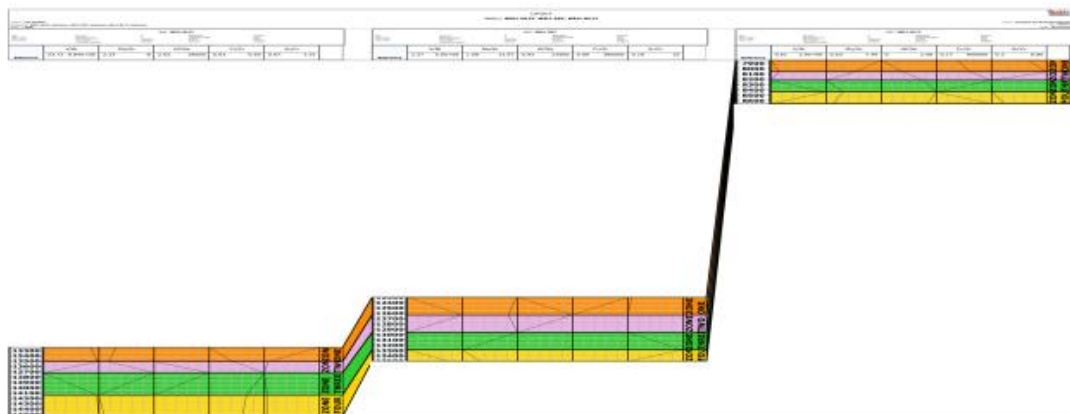


Figure 5: Showing Chemostratigraphic correlation for DS, ML 1 and ML 2 wells, with the plotted geochemical profiles for V/Ni, Mo/Sr, Hf/Ge, Cr/Zr and Sr/Cr. The transversal dotted lines plotted on each track shows the threshold values used to characterize each geochemical zone.

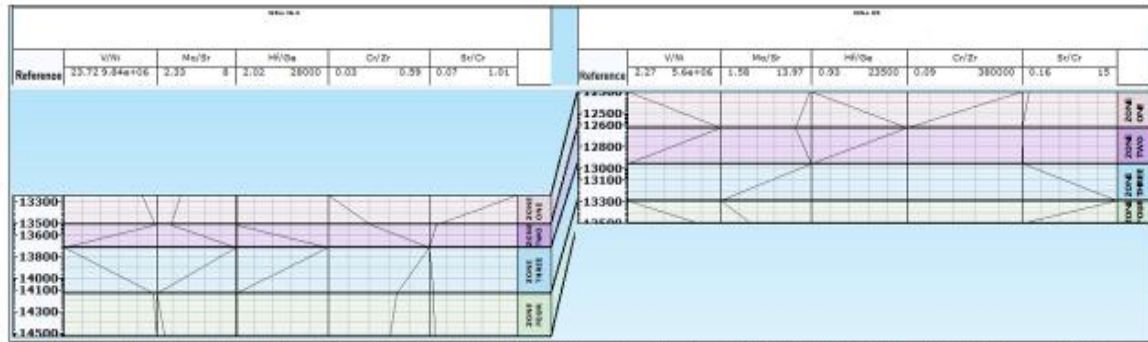


Figure 6: Showing Chemostratigraphic correlation ratio for DS and ML 2 wells, with the plotted geochemical profiles for V/Ni, Mo/Sr, Hf/Ge, Cr/Zr and Sr/Cr. The transversal dotted lines plotted on each track shows the threshold values used to characterize each geochemical zone.

3.9 Zonation confidence

Essentially, pie charts assist in quantifying and displaying the confidence of the zonation. The findings demonstrate how many samples were correctly classified to each zone given the cut off applied in the most important elemental ratio (Figure 7). An average of 76.2 percent data is correctly classified in samples sent into the zone MZ 1. MZ 1 zonation percentage is least in the four types of zoning identified in the study, and that is applicable for the V/Ni greater than 19. The percentage of proxies is the most abundant which displayed the properly classified proxies in the offset wells has the largest percent termed as 92.6 percent by the Cr/Zr, Sr/Cr and Mo/Sr ratios over 90 percent belong entirely to zone M.Z 2. The zone MZ 4 is characterised by general confidence of sample classification of 82.9 percent. Sr/Cr ratio is the most dependable ratio in regard to accurate definition of the zone with 92.1 percentage of the samples having been accurately classified. Zone MZ 3 is very critical since faults in the uncertainty of the geological model might lead to the inadvertent departure of the interest zone during horizontal drilling. In zone MZ 3, zonation confidence represents 91.9 percent, and Cr/Zr, Sr/Cr, Hf/Ge ratios are higher than 90 percent substantiating zonation confidence (Olaru et al., 2018). The level of confidence of the chemostratigraphic zonations is very high because 85.9 percent of the samples are correctly assigned during the pre-application stage (Table.5). These outcomes are also strong due to the high confidence values that are greater than 70% indicating a high degree of zonation confidence (Craigie, 2016).

Table 5: Zonation Confidence for MZ 1, MZ 2, MZ 3 and MZ 4 zones in DS, ML 1 and ML 2 wells.

Zone	Ratio	% zonation confidence		
		Ratio %	Zone	All zones
MZ 1	V/Ni > 15.86	24.23	76.2	100
	Co/Mo > 0.1	0.0		
MZ 2	Si/Zr < 20.0	30.51	100	
	Sr/Ba < 1.5	2.3		
	Th/Sr < 0.1	0.0		
	Co/Mo < 0.1	0.0		
MZ 3	Zr/Sr > 20.0	30.51	100	
	Co/Mo > 0.1	0.0		
	Sr/Ba < 1.5	2.3		
	Th/Sr < 0.1	0.0		
MZ 4	Zr/Sr < 20.0	30.51	100	
	Co/Mo < 0.1	0.0		
	Sr/Ba > 1.5	2.35		
	Th/Sr < 0.1	0.0		

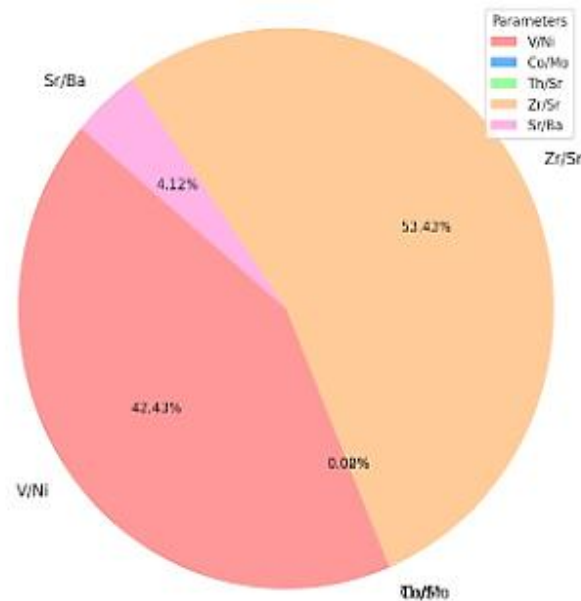


Figure. 7. Pie charts representing the zonation confidence in the defined geochemical zones of the Study Wells

3.10 Chemosteering of the Study Wells

From the low variation in 12,300 ft (0.63) indicates a shale or clay-rich zone which characterizes the elemental ratios profiles of the DS well but at 12,630 ft and 13,500 ft indicate a high ratios value of (4.32-3.94) which suggest clean sandstone, likely good for reservoir targeting. Figure 8, shows that depth 12,960 ft and 13,290 ft in the DS well has Intermediate values ratio of (1.69–2.77) which may represent interbedded sands and shales, possibly transition zones. This implies that the DS well cuts across both shale-dominated and sand-dominated intervals. The high ratios at 12,630 and 13,500 ft are ideal targets for horizontal steering within reservoir-quality sandstone beds. The lower values act as boundary markers or tops of sealing units. Generally, the DS well Shale-rich interval at 12,300 ft with ratio (0.63) is likely deposited in a low-energy, offshore marine or prodelta setting. But the higher values at 12,630 ft with (4.32) ratio and 13,500 ft (3.94) indicate clean sandstone, typical of shoreface to fluvial channel deposits. In a transition zones within the depth range of (12,960, 13,290 ft) Suggest interbedding, possibly delta front or tidal flat environments. The DS well records a transgressive-regressive sequence from low-energy offshore to nearshore fluvial or deltaic sandstones. The geochemical analysis corresponding to ML 2 well within the depth of 13,720 ft shows that it exceptionally high ratio value of (16.47) which implies an extremely quartz-rich sandstone possibly very mature or reworked (Figure. 8). The sharp jump between 13,240 and 13,720 ft suggests a chemostratigraphic boundary or facies change. The consistent >3 ratios from 13,510 ft onward suggest clean sand layers which indicates that ML 2 well traverses a high-quality reservoir interval between 13,510 and 14,530 ft. In depth 13,720 ft layer could mark a key horizon for horizontal placement. It has also a good porosity and permeability characterized by the extreme ratio and the sample lag time together with the analysis time was approximately 1 hours (average rate of penetration was 918 m/h). The geochemical information was also utilized as an appropriate property according to the incident narrated in participation in the drilling decision made Figure 4.59. Extremely high ratio at 13,720 ft (16.47) suggests a very mature quartz arenite, typical of upper fluvial environments, while high values ratio (≥ 3) across all intervals indicates dominance of clean sand but the sharp ratio jump suggests a sequence boundary or major facies change. ML 2 shows a high-energy depositional environment, possibly fluvial channel systems, with reworked sediments and excellent sorting typical of braided river or coastal sand bars. The rich layer is present in all three offset wells, signalled by positive excursion of $\text{SiO}_2/\text{Al}_2\text{O}_3$ ratios (Table 6). Due to the concentration increase, the contents of $\text{SiO}_2/\text{Al}_2\text{O}_3$ ratio are low until it was generally moderate to high ratios, implying sandy intervals dominate at depth 8,440 ft with a ratio of 3.83 which marks a very clean sandstone interval could represent a maximum regressive surface or shoreface channel sand body, possibly the best reservoir horizon for ML 1 well but consistently moderate to high ratios of (1.89–3.83) suggest dominance of sand-sized quartz grains over clays which indicate a progressive winnowing of finer particles, typical of moderate- to high-energy conditions. The consistency across depths of the study wells makes this a more homogeneous unit, aiding predictable lateral geosteering (Figure. 8). Based on geological model, the top of the target formation comes in at 8,220 ft MD (Measured Depth) at ML 1 backed by the geochemical data in confirming the move to drop down the inclination to the 30 (870 to 840). The strategy of overcoming the uncertainty of the geological model by using the geochemical data was effective because the well trajectory hits the reservoir and $\text{SiO}_2/\text{Al}_2\text{O}_3$ ratios excursions on the geosteering log are obvious. At this point, the project team decided to land the well in the case of selecting the cleanest and most continuous unit to land horizontal sections through the reservoir therefore, the real-time mineral detection using $\text{SiO}_2/\text{Al}_2\text{O}_3$ logs during drilling can guide the bit toward cleaner sands and reservoir navigation of high ratios of $\text{SiO}_2/\text{Al}_2\text{O}_3$ mark sweet spots in the reservoir showing a formation boundary identification with sudden changes in ratio help define stratigraphic surfaces. Without geosteering, assuming well path proceeded as planned, the reservoir interval would have been lost (assuming the determination of the trajectory done prior to geosteering), amounting to around 550 m or 55.5 percent of total planned reservoir exposure. The elemental geochemistry contributed to the steering this multi million EUR well with the financial impact of about 0.25 out of the total cost of the well

and 10 percent of the Logging While Drilling (LWD) investigations cost. In the case under consideration, the modification and improvement of chemostratigraphy took a lot of time and money.

Table 6 Showing $\text{SiO}_2/\text{Al}_2\text{O}_3$ Ratio for DS, ML 1, and ML 2, Wells Geosteering Implications

Depth (ft)	Well	$\text{SiO}_2/\text{Al}_2\text{O}_3$
12300	DS	0.63
12630	DS	4.32
12960	DS	2.77
13290	DS	1.69
13500	DS	3.94
7840	ML 1	1.89
8060	ML 1	2.62
8220	ML 1	1.99
8440	ML 1	3.83
8660	ML 1	2.62
13240	ML 2	2.70
13510	ML 2	6.01
13720	ML 2	16.47
14140	ML 2	3.60
14530	ML 2	3.24

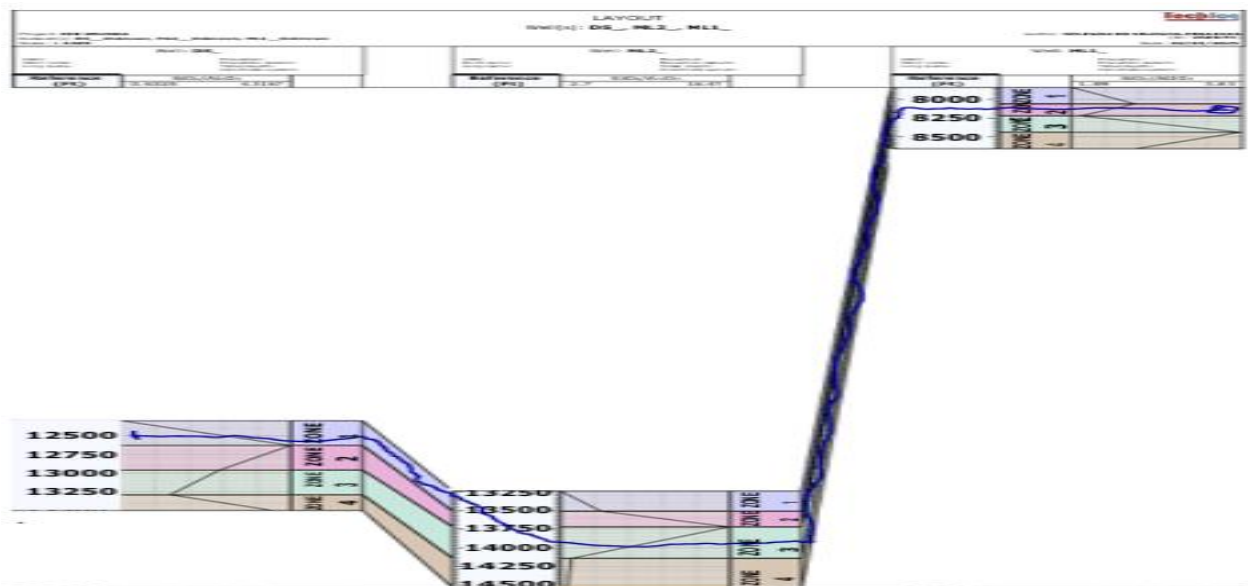


Figure 8: Showing Geosteering Implications for DS and ML 2 wells, with the plotted geochemical profiles for $\text{SiO}_2/\text{Al}_2\text{O}_3$. The transversal blue lines plotted on each track shows the threshold values used to characterize each geochemical zone.

4. CONCLUSIONS

The factors and compositions of elements in defining the chemostratigraphic correlations of unconsolidated siliciclastic reservoirs here mirror provenance shifts and weathering regimes, both expected in most fluvial systems to work out the overview, basinal stratigraphies and processes. The important ratios and components in fingerprinting the reservoir are V/Ni, Mo/Sr, Cr/Zr, Mn, Sr/Cr and Hf/Ge, the depositional environment and the siliciclastic input that control the variation of these ratios. The analysis on x-ray diffraction has shown that the most abundant minerals in the rocks are calcite, kaolinite and quartz. Paleoenvironmental proxies are elements and their abundance as traced by elemental and elemental oxide analysis, with

predominance of SiO_2 , Al_2O_3 and CaO and trace amounts of Cr, V, Ni, Co, Sr, Zn, Zr, Ti and Cd and Ba. Proposed zonation based on chemostratigraphic analysis supports existing descriptions of strata, nevertheless, the quantitative methodology based on ratios used, gives stronger roots to determine correlation and well landing intervals. The success of this in terms of delivering chronostratigraphically significant correlations that contribute value in an oil field context is potentially immeasurable but it will mainly be a factor of the magnitude of the fluvial system compared to the spacing between sections and resolution required of the correlation sought. Applying the geochemical information to bypass the ambiguity of the geological model was successful because the trajectory cuts through the reservoir the excursions of the ratios $\text{SiO}_2/\text{Al}_2\text{O}_3$ are very clear on the geosteering log. At this stage, the project team resorted to landing the well in the event of choosing the cleanest and most continuous unit to land the horizontal sections through the reservoir hence, the real time mineral detection in $\text{SiO}_2/\text{Al}_2\text{O}_3$ logs during drilling can direct the bit at cleaner sands and reservoir navigation by high proportion of $\text{SiO}_2/\text{Al}_2\text{O}_3$ mark sweet spots in the reservoir the formation boundary identification is by the sudden change in ratio may define stratigraphic surfaces. Geochemical model is comprised of four zones including MZ 1, MZ 2, MZ 3 and MZ 4, which are in order of stratigraphic plane. In MZ 1, where $\text{V}/\text{Ni} > 22$, $\text{Mo}/\text{Sr} > 16$. $\text{V}/\text{Ni} > 22$, $\text{Mo}/\text{Sr} < 16$ and $\text{Hf}/\text{Ge} < 27$ are characteristics of MZ2. Zone MZ 3 is related to 2.2 and $\text{V}/\text{Ni} > 22$, whereas MZ 4 brings $\text{V}/\text{Ni} > 22$, $\text{Cr}/\text{Zr} > 2.3$, $\text{Sr}/\text{Cr} < 9$, $\text{Hf}/\text{Ge} < 27$, $\text{Mo}/\text{Sr} < 16$. The suggested zonation on the basis of chemostratigraphic study justifies the already given descriptions of the strata, but the quantitative framework based on presented ratios creates a better basis to outline correlations as well as landing depths of wells. The 85.9 percentage and 89.4 percentage guarantees the zonation confidence of the three wells considered during the pre-application step and the real-time application, respectively. Therefore, distribution of the validity of the geochemical model pre and post real time use. Thus, this practice of chemostratigraphy holds immense prospect of geosteering in real time not just in the Niger Delta Basin but also in any resource play of whatever age spread across the World. Thus, this chemostratigraphic application has immense potential in real-time geosteering not only Niger Delta Basin, but also in any resource play of whatever age anywhere in the World. Hence, this use of chemostratigraphy possesses significant potential in geosteering in real-time, the total expenditure of this application is 0.15 percent of the overall project expenditure, and the cost is 10 percent of the Logging While Drilling (LWD), the price. The method was highly valuable because of the negligible cost thus the application will be an established strategy in subsequent drilling campaigns.

Conflicts of Interest: The authors declare no conflict of interest.

References

- Avbovbo, A.A., (1978). Tertiary lithostratigraphy of Niger Delta. American Association of Petroleum Geologists Bulletin, 62, 295-300.
- Childress, M., and Grammer, G.M., (2015). High resolution sequence stratigraphic architecture of a Mid-Continent Mississippian outcrop in Southwest Missouri: Shale Shaker (August 2015) p. 206-234.
- Craigie, N. (2018). Principles of Elemental chemostratigraphy: A Practical User Guide. New York, NY: Springer International Publishing, 189p
- Craigie, N.W., Pierre, B. and Ahmed, K., (2016). Chemostratigraphy and biostratigraphy of Devonian, Carboniferous and Permian sediments encountered in the eastern Saudi Arabia: An integrated approach to reservoir correlation. Marine and Petroleum Geology, 72, 156-178. DOI: 10.1016/j.marpetgeo.2016.01.018.
- Ejedawe, J.E., Coker, S.J.L., Lambert-Alkhionbare, D.O., Aloof, K.B. and Adult, F.O., (1984). Evolution of oil generation window and oil and gas occurrence in Tertiary Niger Delta Basin. American Association of Petroleum Geologists Bulletin, 68, 1744-1751.
- Evamy, B.D., Haremboure, J., Kamerling, P., Knaap, W.A., Molloy, F.A. and Rowlands, P.H., (1978). Hydrocarbon habitat of Tertiary Niger Delta: American Association of Petroleum Geologists Bulletin, 62, 277- 298.
- Frankl, E.J. and Cordry, E.A., (1967). The Niger Delta oil province: recent developments onshore and offshore. Proceedings of 7th World Petroleum Congress, Mexico City, Mexico, April 2-9, 1967, pp. 125-209.
- Haack, R.C., Sunderaman, P., Diedjomahor, J.O., Xiao, H., Gant, N.J., May, E.D. and Kelsch, K., (2000). Niger delta petroleum system, Nigeria. In: M.R. Mello and B.J Kat, eds. Petroleum Systems of South Atlantic Margins. Tulsa: American Association of Petroleum Geologist, pp. 213-231.
- Ikanne, R., Akintola, I., Bankole, I., Ajibade, M. and Edword, O., (2014). Chemostratigraphic Characterization of Siliciclastic Rocks In Parts of The Eastern Dahomey Basin Southwestern Nigeria. *Journal of Geography and Geology* 6 (4): 88-108.
- Mazzullo, S.J., Boardman, D.R., Wilhite, B.W., Godwin, G., and Morris, B.T., (2013). Revisions of outcrop lithostratigraphic nomenclature in the lower to middle Mississippian subsystem (Kinderhookian to basal Meramecian series) along the shelf-edge in southwest Missouri, northwest Arkansas, and northeast Oklahoma: Shale Shaker, v.63, no.6, p.414-454.
- McLennan, S. M., Bock, B., Hemming, S. R., Hurowitz, J. A., Steven, M. L., and McDaniel, D. K., (2001). "The roles of provenance and sedimentary processes in the geochemistry of sedimentary rocks," in *Geochemistry of sediments and sedimentary rocks/evolutionary considerations to mineral deposit-forming environments*. Editor D. R. Lentz (Canada: Geological Association of Canada), 4, 1-6.
- Mejia, C., Nardi, G. and Iain, D., (2018). Integration of LWD and geochemistry from cuttings measurements for well placement based on real time diagenesis characterization. Offshore Technology Conference, Houston, Texas, April 30-May 3, 2018, DOI: 10.4043/29040-MS.
- North, C. P., Hole, M. J., and Jones, D. G., (2005). Geochemical correlation in deltaic successions; a reality check: Geological Society of America Bulletin, v. 117 (5-6), p. 620-632.

- Olaru R., Krézsek C., Rainer T.M., Ungureanu C., Turi V., Ionescu G., and Tari G., (2018). 3D basin modelling of Oligocene Miocene Maikop source rocks offshore Romania and in the Western Black Sea, *J. Pet. Geol.* 41, 351–365. <https://doi.org/10.1111/jpg.12707>.
- Prundeanu, I.M., Chelariu, C. and Perez, D.R.C., (2021). Elemental geochemistry of the upper cretaceous reservoir and surrounding formations applied in geosteering of horizontal wells, Lebăda Field – Western Black Sea. *Oil & Gas Science and Technology- Revue d'IFP Energies Nouvelles*, 76, DOI: 10.2516/ogst/2020083.
- Ramkumar, M., (2015). *Chemostratigraphy: Concepts, Techniques, and Applications*; Elsevier: Amsterdam, The Netherlands, pp. 1–432.
- Ratcliffe, K. T., Wright, A. M. and Spain, D., (2012). Unconventional Methods For Unconventional Plays: Using Elemental Data To Understand Shale Resource Plays: *PESA News Resources*, March / April 2012, p. 89-93.
- Reijers, T.J.A., (2011). Stratigraphy and sedimentology of the Niger Delta. *Geologos*, 17(3), 133-162, DOI: 10.2478/v10118-011-0008-3.
- Short, K.C. and Stauble, A.J., (1967). Outline geology of Niger Delta. *American Association of Petroleum Geologists Bulletin*, 51, 761-779.
- Taylor, S. R. and McLennan, S. M., (1985). *The Continental Crust: its Composition and Evolution: An Examination of the Geological Record Preserved in Sedimentary Rocks*: Blackwell, Oxford, U.K. 328.
- Weber, K.J. and Daukoru, E.M., (1975). Petroleum geology of the Niger Delta. In: *Proceedings of the 9th World Petroleum Congress*, Tokyo, Japan, May 11-16, 1975, pp. 210-221.